

Neutrino magnetic moments: effective versus fundamental parameters

Christoph A. Ternes ^{1, a} and Mariam Tórtola ^{2, 3, b}

¹*Istituto Nazionale di Fisica Nucleare (INFN),*

Laboratori Nazionali del Gran Sasso, 67100 Assergi, L'Aquila (AQ), Italy

²*Instituto de Física Corpuscular (CSIC-Universitat de València),*

Parc Científic UV C/ Catedrático José Beltrán, 2 E-46980 Paterna (Valencia), Spain

³*Departament de Física Teòrica, Universitat de València, Spain*

The search for neutrino magnetic moments offers a valuable window into physics beyond the Standard Model. However, a common misconception arises in the interpretation of experimental results: the assumption that the so-called effective neutrino magnetic moment is a universal, experiment-independent quantity. In reality, this effective parameter depends on the specific characteristics of each experiment, including the neutrino source, flavor composition or energy spectrum. As a result, the effective magnetic moment derived from solar neutrino data differs fundamentally from that obtained in reactor or accelerator-based experiments. Treating these quantities as directly comparable can lead to misleading conclusions. In this work, we clarify the proper definition of the effective neutrino magnetic moment in various experimental contexts and discuss the implications of this misconception for global analyses and theoretical interpretations.

Keywords: electromagnetic properties, solar neutrinos, reactor neutrinos, neutrino oscillations

I. INTRODUCTION

In recent years, neutrino electromagnetic properties [1–4] have become a subject of intense research. Both experimental collaborations [5–14] and phenomenologists [15–28] have analyzed available data in search of signs of such properties. Particular attention has been given to neutrino magnetic and electric transition and dipole moments, which can arise in many extensions of the Standard Model (SM) that account for neutrino masses [29]. The sensitivities achieved in current experiments remain several orders of magnitude above the values predicted by the minimal extension of the SM with right-handed Dirac neutrinos [3, 30, 31]. Nevertheless, in more sophisticated theoretical frameworks -see, for example, Ref. [32]- the predicted neutrino magnetic moments can be significantly larger and may be within reach of current or upcoming experimental efforts. For a comprehensive overview, see the review in [29].

Neutrino electromagnetic properties are typically probed by searching for deviations in the low-energy spectra of experiments that measure nuclear or electron recoils via coherent elastic neutrino-nucleus scattering (CE ν NS) or elastic neutrino-electron scattering (E ν ES), respectively. Due to the helicity flipping nature of the interaction, the magnetic moment contribution adds incoherently to the SM cross sections, leading to a characteristic enhancement at low energies. The magnetic moment cross section is given by [33]

$$\left. \frac{d\sigma}{dT} \right|^{MM} \propto \frac{\pi \alpha_{EM}^2}{m_e^2} \left(\frac{1}{T} - \frac{1}{E_\nu} \right) \left| \frac{\mu_{\nu_\ell}}{\mu_B} \right|^2, \quad (1)$$

where α_{EM} is the fine-structure constant, m_e the electron mass, T the nuclear or electron recoil energy, E_ν the neutrino energy, μ_{ν_ℓ} is the effective magnetic moment for ν_ℓ , and $\mu_B = e/(2m_e)$ is

^a christoph.ternes@lngs.infn.it

^b mariam@ific.uv.es

the Bohr magneton. In the case of CE ν NS experiments, this cross section must be multiplied by the nuclear form factor and the proton number squared, whereas in E ν ES experiments, it is scaled by the effective number of ionizable electrons.

Experimental data are commonly used to set limits on the effective neutrino magnetic moment, $\mu_{\nu\ell}$. These bounds are often compared across different experiments and neutrino flavors, without recognizing that $\mu_{\nu\ell}$ is not a fundamental quantity. Instead, it is an effective parameter that depends on several factors, including the experimental setup, the neutrino energy spectrum, the neutrino flavor, and even whether neutrinos are Dirac or Majorana particles. This issue has been previously discussed in the literature (see, e.g., Refs. [34, 35] and the recent Ref. [36]), yet some confusion persists in the field. The aim of this article is to clarify the connections among the different effective magnetic moments $\mu_{\nu\ell}$ and to update the bounds on the underlying physical parameters, which are independent of experimental assumptions. Based on the most stringent limits on these fundamental parameters, we define a benchmark "playground" that future experiments must reach in order to surpass current constraints.

The paper is structured as follows: In Section II we introduce our notation and explain how the effective magnetic moments are related to the underlying fundamental parameters. Section III reviews the constraints obtained from different experimental setups. In Section IV we use the most stringent bounds on the fundamental parameters to derive limits on the individual effective magnetic moments. Finally, Section V presents our conclusions.

II. THEORETICAL FRAMEWORK

The effective Hamiltonian that accounts for electromagnetic interactions depends on the Majorana or Dirac nature of neutrinos. In this paper, we will mainly be interested in Majorana neutrinos. In this case, the Hamiltonian can be written as [1, 37]

$$H_{\text{EM}}^{\text{M}} = -\frac{1}{4}\nu_L^{\text{T}}C^{-1}\lambda^{\text{M}}\sigma^{\alpha\beta}\nu_L F_{\alpha\beta} + \text{h.c.}, \quad (2)$$

where $F_{\alpha\beta}$ is the electromagnetic field tensor, $\lambda^{\text{M}} = \mu^{\text{M}} - id^{\text{M}}$ is an antisymmetric complex matrix, with μ^{M} and d^{M} being the magnetic and electric moments for Majorana neutrinos. Due to its antisymmetric nature, λ^{M} is characterized by three complex (or six real) parameters. The corresponding Hamiltonian for the case of Dirac neutrinos is instead given by

$$H_{\text{EM}}^{\text{D}} = \frac{1}{2}\bar{\nu}_R\lambda^{\text{D}}\sigma^{\alpha\beta}\nu_L F_{\alpha\beta} + \text{h.c.} \quad (3)$$

This time, $\lambda^{\text{D}} = \mu^{\text{D}} - id^{\text{D}}$ is an arbitrary complex matrix, restricted only to the hermiticity of the Hamiltonian, implying $\mu^{\text{D}} = (\mu^{\text{D}})^{\dagger}$ and $d^{\text{D}} = (d^{\text{D}})^{\dagger}$. Note that, due to the different structure of the Hamiltonian, neutrino electromagnetic properties can potentially be used to distinguish between the Dirac and Majorana neutrino nature. A key difference lies in the antisymmetric nature of λ^{M} for Majorana neutrinos, which enforces vanishing diagonal elements: $\mu_{ii}^{\text{M}} = d_{ii}^{\text{M}} = 0$. In contrast, for Dirac neutrinos, diagonal magnetic and electric dipole moments are allowed. Numerical estimates for the magnetic and electric moments have been obtained within the minimal $\text{SU}(2)_{\text{L}} \otimes \text{U}(1)_{\text{Y}}$ model [3]. In this scenario, however, the predicted values are extremely small, well below the reach of current and near-future neutrino experiments. In contrast, in extended models beyond the SM, significantly larger moments can arise, with values potentially within the sensitivity range of present or upcoming experiments [29, 32]. In this work, we remain agnostic about the specific underlying model that generates these moments and focus on the study of Majorana transition magnetic moments (TMM), denoted by μ_{ij}^{M} . For simplicity, we will omit the superscript "M" referring to Majorana neutrinos from here on.

The effective neutrino magnetic moment observed in a given experiment depends on the underlying neutrino magnetic moment matrix and the amplitudes of the positive and negative helicity neutrino states, denoted by the three-component vectors a_+ and a_- , respectively. In the flavor basis, one finds [38]

$$\left(\mu_\nu^F\right)^2 = a_-^\dagger \lambda^\dagger \lambda a_- + a_+^\dagger \lambda \lambda^\dagger a_+, \quad (4)$$

where λ is the TMM matrix in the flavor basis. In the mass basis, the TMM matrix, $\tilde{\lambda}$, as well as the corresponding three-component neutrino vector states, \tilde{a}_- and \tilde{a}_+ , can be obtained from the following transformations

$$\tilde{a}_- = U^\dagger a_-, \quad \tilde{a}_+ = U^T a_+, \quad \tilde{\lambda} = U^T \lambda U, \quad (5)$$

where U is the leptonic mixing matrix. With these elements one can define the effective neutrino magnetic moment in the mass basis as [34],

$$\left(\mu_\nu^M\right)^2 = \tilde{a}_-^\dagger \tilde{\lambda}^\dagger \tilde{\lambda} \tilde{a}_- + \tilde{a}_+^\dagger \tilde{\lambda} \tilde{\lambda}^\dagger \tilde{a}_+, \quad (6)$$

As mentioned above, three complex quantities are required to parametrize the TMM, so we can write the TMM matrices in the flavour and mass basis as

$$\lambda = \begin{pmatrix} 0 & \Lambda_\tau & -\Lambda_\mu \\ -\Lambda_\tau & 0 & \Lambda_e \\ \Lambda_\mu & -\Lambda_e & 0 \end{pmatrix}, \quad \tilde{\lambda} = \begin{pmatrix} 0 & \Lambda_3 & -\Lambda_2 \\ -\Lambda_3 & 0 & \Lambda_1 \\ \Lambda_2 & -\Lambda_1 & 0 \end{pmatrix}, \quad (7)$$

where we have introduced the complex parameters [34]

$$\Lambda_\alpha = |\Lambda_\alpha| e^{i\varphi_\alpha}, \quad \Lambda_i = |\Lambda_i| e^{i\varphi_i}. \quad (8)$$

As argued in Ref. [38], among the six CP-violating phases that appear in the neutrino mixing matrix and the TMM matrix, only three are physically relevant. Following the convention adopted in Refs. [35, 36], together with the δ_{CP} phase in the neutrino mixing matrix, we consider only two of the phases φ_i to be non-zero and assume Λ_2 to be a real parameter.

Note that, although we have presented two equivalent expressions for the effective magnetic moment -Eqs. (4) and (6)- in the flavour and mass bases, respectively, the quantity itself is, of course, basis-independent. However, it is evident from those expressions that the specific value of the effective magnetic moment depends on the characteristics of each experimental setup. In the next section, when discussing the bounds from different experiments, we will highlight some of these differences.

III. EXPERIMENTAL BOUNDS ON NEUTRINO MAGNETIC MOMENTS

In this section, we review the most relevant bounds on neutrino magnetic moments reported in the literature. In all cases, we translate the experimental limits on the effective parameter into constraints on the fundamental quantities that enter the Hamiltonian. Our focus is on the most stringent bounds obtained from short-baseline (SBL) reactor and accelerator experiments, solar neutrino observations, and dark matter direct detection (DMDD) experiments. Additional, complementary constraints have been derived from CE ν NS measurements in Refs. [18–20, 22, 23, 26–28]. Note, however, that the resulting limits are currently at least an order of magnitude weaker than those discussed here. On the other hand, astrophysical observations provide some of the most

stringent constraints on the neutrino magnetic moment. These arise from enhanced energy-loss processes in stellar environments, where a non-zero magnetic moment would increase neutrino emission rates (see, e.g., [39]). Such bounds are often not emphasized in phenomenological studies focused on terrestrial experiments, as they rely on specific astrophysical models and assumptions that may introduce additional uncertainties. Nonetheless, with DMDD experiments now reaching comparable sensitivities, the omission of astrophysical limits becomes less critical in this context. A comprehensive list of current bounds on effective magnetic moments can be found in Ref. [40].

In Section III A, we present the leading bounds obtained from SBL neutrino experiments, specifically GEMMA and LSND. Section III B focuses in constraints from DMDD experiments, which are sensitive to solar neutrinos: these are compared with the bounds from Borexino. For GEMMA, LSND and Borexino we reinterpret the limits on the effective magnetic moments previously obtained in terms of the fundamental parameters entering the Hamiltonian. In contrast, for DMDD experiments we perform a direct fit to the experimental data. In all analyses below, we minimize over the standard neutrino oscillation parameters incorporating their uncertainties as reported in Ref. [41]. Additionally, the new CP-violating phases φ_1 and φ_3 , as well as the (not displayed) Λ parameter, are treated as free parameters and marginalized over in the fits.

A. Bounds from short-baseline experiments

We begin our discussion with the results from short-baseline experiments, focusing on GEMMA and LSND. GEMMA [11] was a reactor-based neutrino experiment designed to search for neutrino magnetic moments. It operated at the Kalinin Nuclear Power Plant in Russia, approximately 13.9 m from the core of a 3 GW pressurized water reactor. GEMMA employed a high-purity germanium detector with an active mass of about 1.5 kg, optimized to detect low-energy electron recoils resulting from $E\nu$ ES. On the other hand, the Liquid Scintillator Neutrino Experiment (LSND) [7] was conducted at Los Alamos National Laboratory between 1993 and 1998, primarily aimed at searching for short-baseline neutrino oscillations. The experiment used an 800 MeV proton beam to produce pions, which decayed to μ^+ and ν_μ , followed by μ^+ decays into e^+ , ν_e and $\bar{\nu}_\mu$. As a result, the neutrino beam in LSND consisted of ν_μ , $\bar{\nu}_\mu$ and ν_e . The detector was sensitive to both $E\nu$ ES and inverse beta decay events. At 90% confidence level (CL) the respective collaborations reported the following bounds on the effective neutrino magnetic moment

$$\mu_\nu < 2.9 \times 10^{-11} \mu_B \quad (\text{GEMMA}), \quad (9)$$

$$\mu_\nu < 6.8 \times 10^{-10} \mu_B \quad (\text{LSND}). \quad (10)$$

In the flavor basis, the effective Majorana TMM relevant for a SBL reactor experiment, with $a_-^T = (0, 0, 0)$ and $a_+^T = (1, 0, 0)$, is given by [34]

$$\left(\mu_{\nu, \text{reactor}}^F\right)^2 = |\Lambda_\mu|^2 + |\Lambda_\tau|^2, \quad (11)$$

where $|\Lambda_\mu|$ and $|\Lambda_\tau|$ are the elements of the neutrino TMM matrix λ in Eq. (7). For LSND, the flavour composition of the neutrino flux implies $a_-^T = (1, 1, 0)$ and $a_+^T = (0, 1, 0)$. The resulting effective magnetic moment in the flavor basis is [34]

$$\left(\mu_{\nu, \text{acceler}}^F\right)^2 = |\mathbf{\Lambda}|^2 + |\Lambda_e|^2 + 2|\Lambda_\tau|^2 - 2|\Lambda_e||\Lambda_\mu| \cos(\varphi_e - \varphi_\mu), \quad (12)$$

where $|\mathbf{\Lambda}|^2 = |\Lambda_e|^2 + |\Lambda_\mu|^2 + |\Lambda_\tau|^2 = |\Lambda_1|^2 + |\Lambda_2|^2 + |\Lambda_3|^2$. In the mass basis, these expressions become significantly more complex due to their dependence on the neutrino mixing parameters. For completeness, we refer the reader to Ref. [35], where the full expressions are provided. As

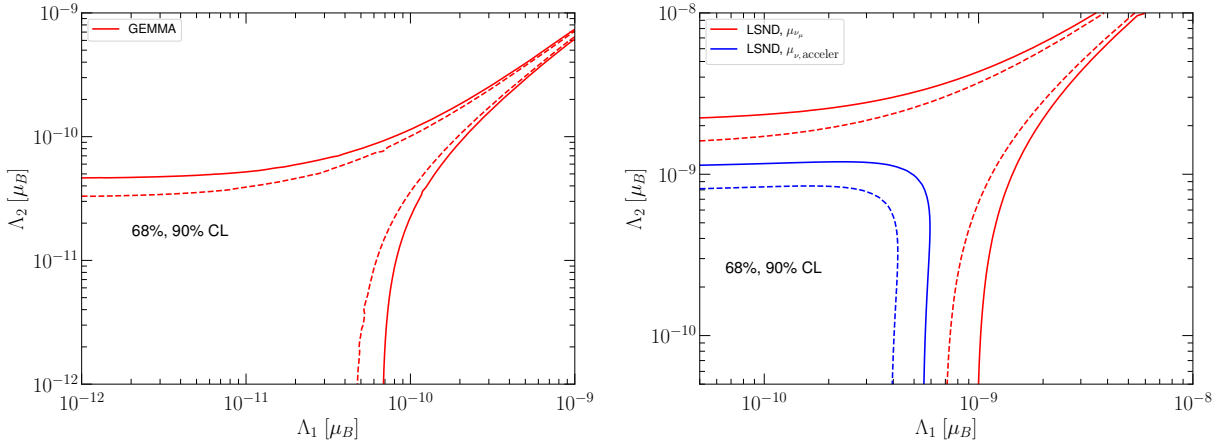


FIG. 1: The 1σ (dashed) and 90% CL (solid lines) contours in the $\Lambda_1 - \Lambda_2$ obtained from GEMMA (left) and LSND (right) data. The LSND region is represented for two different assumptions for the effective magnetic moment. The blind spot region for LSND is only present if one attributes the effective magnetic moment only to ν_μ .

evident from Eqs. (11) and (12), the expressions for the effective magnetic moments differ in their dependence on the fundamental parameters. They should therefore not be directly compared.

In the left panel of Fig. 1 we present the results from GEMMA [11] in the $\Lambda_1 - \Lambda_2$ plane¹ showing the 1σ and 90% CL regions for two degrees of freedom. As can be seen, cancellations among the fundamental parameters are possible, potentially leading to blind spots, where even sizeable transition magnetic moments Λ_i result in small effective magnetic moments in the case of for reactor neutrinos. These cancellations occur when the CP-violating phases satisfy $\varphi_1 \approx 0$ and $\varphi_3 \approx \pi$, a feature previously identified and discussed in Ref. [36]. In that study, the authors also identified a blind spot for LSND. However, it arises only under the assumption that the entire effective magnetic moment originates from interactions involving muon neutrinos. In that case, the effective magnetic moment is given by

$$\left(\mu_{\nu_\mu}^F\right)^2 = |\Lambda_e|^2 + |\Lambda_\tau|^2. \quad (13)$$

In this case, achieving a blind spot requires the CP-violating phases to be $\varphi_1 = \pi$ and $\varphi_3 = 0$, opposite to the conditions for reactor neutrinos. As a result, a combined analysis of GEMMA and LSND data cannot simultaneously access blind spots in both experiments. In any case, once the full composition of the LSND neutrino beam—comprising ν_μ , $\bar{\nu}_\mu$, and ν_e —is properly taken into account, the degeneracy is lifted and the blind spot vanishes. This effect is illustrated in the right panel of Fig. 1, where we compare the confidence contours obtained assuming a pure ν_μ beam (red lines) with those from the realistic mixed beam (blue lines).

B. Bounds from solar neutrinos

For solar neutrinos, effective magnetic moments can be probed through elastic scattering with electrons in detectors such as Super-Kamiokande, Borexino, and also in dark matter direct detection experiments. The analysis of the recoil electron energy spectrum from solar neutrino scattering

¹ Similar contours can be obtained for other combinations of Λ parameters in both experiments

provides a powerful tool to constrain the neutrino magnetic moment. Such analyses have been carried out using data from Super-Kamiokande [34] and Borexino [12, 24, 35]. In particular, Borexino achieved an order-of-magnitude improvement over previous solar constraints thanks to its sensitivity to lower-energy neutrinos, where the impact of TMMS is more pronounced. When deriving the effective magnetic moment in this context, it is essential to account for the fact that neutrinos reach Earth as an incoherent mixture of mass eigenstates due to flavor oscillations during their propagation from the Sun. In the mass basis, the effective neutrino magnetic moment is expressed as [34]

$$(\mu_{\text{sol}}^M)^2 = |\mathbf{\Lambda}|^2 - c_{13}^2 |\Lambda_2|^2 + (c_{13}^2 - 1) |\Lambda_3|^2 + c_{13}^2 P_{e1}^{2\nu} (|\Lambda_2|^2 - |\Lambda_1|^2), \quad (14)$$

where $P_{e1}^{2\nu}$ is the effective two-neutrino oscillation probability for solar neutrinos. Note that this expression does not depend on any of the phases of the TMM matrix, as has already been noticed before [34].

In this section, we also examine the bounds derived from the analysis of data from DMDD experiments, in particular XENONnT [14], LUX-ZEPLIN (LZ) [42] and PandaX-4T [43]. Following the approach in [25], we perform a direct fit to the fundamental parameters rather than to the effective magnetic moment. The result of the combined analysis of all three experiments is shown in Fig. 2. The left panel displays the 1σ and 90% CL allowed regions (for two degrees of freedom) in the $\Lambda_1 - \Lambda_2$ (blue) and $\Lambda_1 - \Lambda_3$ (red) planes. As previously noted, the effective magnetic moment for solar neutrinos is independent of the CP-violating phases, and thus no cancellations can happen among the parameters. Overall, the bounds obtained here are stronger than those from the short-baseline experiments GEMMA or LSND, discussed earlier, and they also improve upon previous solar neutrino limits from Super-Kamiokande and Borexino. The right panel shows the $\Delta\chi^2$ profiles for the individual Λ_i , along with a comparison to Borexino-based bounds [24] (dashed lines). These results highlight that the lower energy thresholds of DMDD experiments allow them to set stronger constraints than dedicated solar neutrino experiments. The bounds from DMDD experiments at 90% CL read

$$\Lambda_1 < 1.3 \times 10^{-11} \mu_B, \quad (15)$$

$$\Lambda_2 < 0.9 \times 10^{-11} \mu_B, \quad (16)$$

$$\Lambda_3 < 0.8 \times 10^{-11} \mu_B, \quad (17)$$

and update those reported in Ref. [36] which were based on earlier data from XENON-1T [44]. In the next section we will use these updated constraints to infer the corresponding values of the effective magnetic moments relevant for other experimental setups.

IV. IMPLICATIONS FOR REACTOR AND ACCELERATOR EXPERIMENTS

We now turn to the interpretation of our results. We use the stringent bounds on the fundamental parameters Λ_i , derived from DMDD experiments, to infer the corresponding limits on the effective magnetic moments relevant for SBL reactor and accelerator experiments. These translated constraints are shown in Fig. 3, and serve to illustrate how bounds on the underlying parameters map onto observables in different experimental contexts. At 90% confidence level, the bounds read

$$\mu_{\nu, \text{reactor}} < 1.0 \times 10^{-11} \mu_B, \quad (18)$$

$$\mu_{\nu, \text{acceler}} < 2.1 \times 10^{-11} \mu_B. \quad (19)$$

This implies that current and upcoming searches at reactor and accelerator facilities must improve their sensitivity to compete with those based on solar neutrino data. For comparison, the bound

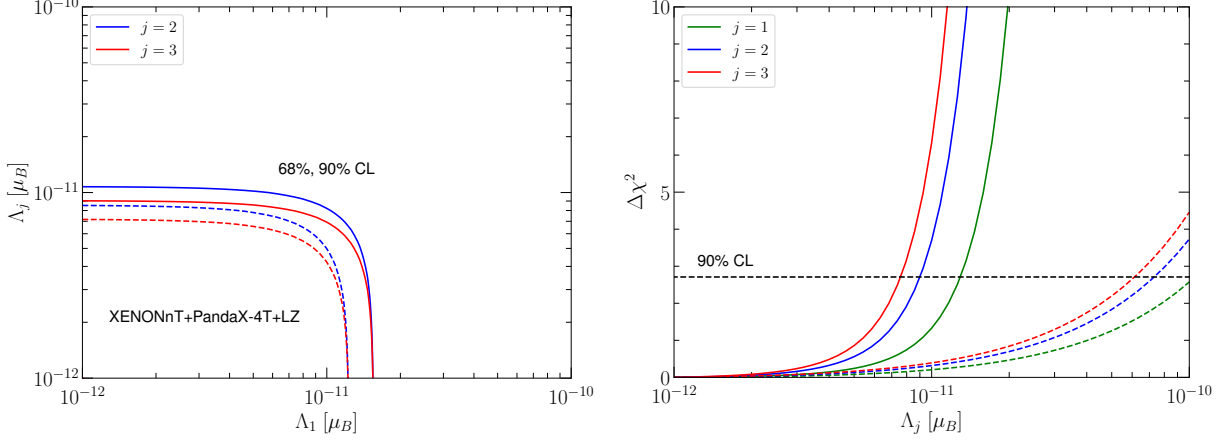


FIG. 2: Left: The 1σ (dashed line) and 90% (solid line) contours in the $\Lambda_1 - \Lambda_j$ plane obtained from DMDD data. Right: The corresponding $\Delta\chi^2$ profiles (solid) for the individual Λ_j . Also shown for comparison the bounds from Borexino (dashed).

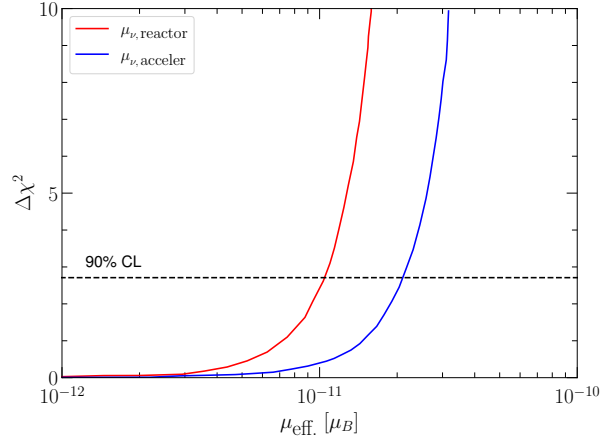


FIG. 3: Constraints on the effective neutrino magnetic moments in reactor and accelerator experiments, derived from the bounds on the fundamental parameters Λ_i obtained in DMDD experiments.

derived from solar neutrino observations is $\mu_{\text{sol}} < 7.5 \times 10^{-12}, \mu_B$ [25], which remains more stringent than the values currently accessible in terrestrial setups. Nevertheless, it should be noted that, even if future experiments reach similar sensitivities, combined analyses involving reactor, accelerator and solar neutrino experiments will remain essential. Such a joint approach is crucial to resolve the parameter degeneracies inherent in the definition of μ_ν and to eliminate blind spots in the Λ_i parameter space.

V. CONCLUSIONS

In this work, we have aimed to clarify persistent misconceptions within the community regarding the interpretation of neutrino magnetic moment bounds. In particular, we have demonstrated how the effective magnetic moment is experiment-dependent, differing in its form for reactor, accelerator, and solar neutrino setups. We have updated the constraints on the fundamental

transition magnetic moments of Majorana neutrinos using the latest results from dark matter direct detection experiments. Thanks to their low energy thresholds, these experiments, which receive an irreducible background contribution from solar neutrinos, achieve stronger bounds than dedicated solar neutrino detectors such as Borexino. These updated bounds on the fundamental parameters were then used to derive the corresponding constraints on the effective magnetic moments relevant for reactor and accelerator neutrino experiments. As shown in Section IV, the effective magnetic moments inferred from DMDD limits differ significantly from the direct bound on μ_{sol} . Therefore, it is this translated value—not the solar neutrino limit itself—that should be used as a benchmark when evaluating or comparing reactor and accelerator constraints or experimental sensitivities, contrary to common practice in the literature. Finally, note that, while our study has focused on transition magnetic moments for Majorana neutrinos, the same analysis can be straightforwardly extended to the Dirac case, with appropriate modifications to account for the different structure of their magnetic moment matrices [36]. This highlights the general relevance of our results and the need for careful interpretation of experimental bounds across different neutrino frameworks.

ACKNOWLEDGMENTS

We would like to thank Dimitris Papoulias and Gonzalo Sánchez García for helpful discussions. Work supported by the Spanish grants PID2023-147306NB-I00 and CEX2023-001292-S (MCIU/AEI/ 10.13039/501100011033) and CIPROM/2021/054 from Generalitat Valenciana.

-
- [1] J. Schechter and J. W. F. Valle, “Majorana Neutrinos and Magnetic Fields,” *Phys. Rev. D* **24** (1981) 1883–1889. [Erratum: *Phys.Rev.D* 25, 283 (1982)].
 - [2] J. F. Nieves, “Electromagnetic Properties of Majorana Neutrinos,” *Phys. Rev. D* **26** (1982) 3152.
 - [3] R. E. Shrock, “Electromagnetic properties and decays of Dirac and Majorana neutrinos in a general class of gauge theories,” *Nucl. Phys.* **B206** (1982) 359.
 - [4] B. Kayser, “Majorana Neutrinos and their Electromagnetic Properties,” *Phys. Rev. D* **26** (1982) 1662.
 - [5] L. A. Ahrens *et al.*, “Determination of electroweak parameters from the elastic scattering of muon-neutrinos and anti-neutrinos on electrons,” *Phys. Rev. D* **41** (1990) 3297–3316.
 - [6] R. C. Allen *et al.*, “Study of electron-neutrino electron elastic scattering at LAMPF,” *Phys. Rev. D* **47** (1993) 11–28.
 - [7] **LSND** Collaboration, L. B. Auerbach *et al.*, “Measurement of electron - neutrino - electron elastic scattering,” *Phys. Rev. D* **63** (2001) 112001, [arXiv:hep-ex/0101039](#).
 - [8] **DONUT** Collaboration, R. Schwienhorst *et al.*, “A New upper limit for the tau - neutrino magnetic moment,” *Phys. Lett. B* **513** (2001) 23–29, [arXiv:hep-ex/0102026](#).
 - [9] **MUNU** Collaboration, Z. Daraktchieva *et al.*, “Final results on the neutrino magnetic moment from the MUNU experiment,” *Phys. Lett. B* **615** (2005) 153–159, [arXiv:hep-ex/0502037](#).
 - [10] **TEXONO** Collaboration, H. T. Wong *et al.*, “A Search of Neutrino Magnetic Moments with a High-Purity Germanium Detector at the Kuo-Sheng Nuclear Power Station,” *Phys. Rev. D* **75** (2007) 012001, [arXiv:hep-ex/0605006](#).
 - [11] A. G. Beda, V. B. Brudanin, V. G. Egorov, D. V. Medvedev, V. S. Pogosov, M. V. Shirchenko, and A. S. Starostin, “The results of search for the neutrino magnetic moment in GEMMA experiment,” *Adv. High Energy Phys.* **2012** (2012) 350150.
 - [12] **Borexino** Collaboration, M. Agostini *et al.*, “Limiting neutrino magnetic moments with Borexino Phase-II solar neutrino data,” *Phys. Rev. D* **96** no. 9, (2017) 091103, [arXiv:1707.09355 \[hep-ex\]](#).
 - [13] **PandaX-II** Collaboration, X. Zhou *et al.*, “A Search for Solar Axions and Anomalous Neutrino Magnetic Moment with the Complete PandaX-II Data,” *Chin. Phys. Lett.* **38** no. 1, (2021) 011301, [arXiv:2008.06485 \[hep-ex\]](#). [Erratum: *Chin.Phys.Lett.* 38, 109902 (2021)].

- [14] **XENON** Collaboration, E. Aprile *et al.*, “Search for New Physics in Electronic Recoil Data from XENONnT,” *Phys. Rev. Lett.* **129** no. 16, (2022) 161805, [arXiv:2207.11330 \[hep-ex\]](#).
- [15] M. Atzori Corona, W. M. Bonivento, M. Cadeddu, N. Cargioli, and F. Dordei, “New constraint on neutrino magnetic moment and neutrino millicharge from LUX-ZEPLIN dark matter search results,” *Phys. Rev. D* **107** no. 5, (2023) 053001, [arXiv:2207.05036 \[hep-ph\]](#).
- [16] S. K. A., A. Majumdar, D. K. Papoulias, H. Prajapati, and R. Srivastava, “Implications of first LZ and XENONnT results: A comparative study of neutrino properties and light mediators,” *Phys. Lett. B* **839** (2023) 137742, [arXiv:2208.06415 \[hep-ph\]](#).
- [17] A. N. Khan, “Light new physics and neutrino electromagnetic interactions in XENONnT,” *Phys. Lett. B* **837** (2023) 137650, [arXiv:2208.02144 \[hep-ph\]](#).
- [18] M. Atzori Corona, M. Cadeddu, N. Cargioli, F. Dordei, C. Giunti, Y. F. Li, C. A. Ternes, and Y. Y. Zhang, “Impact of the Dresden-II and COHERENT neutrino scattering data on neutrino electromagnetic properties and electroweak physics,” *JHEP* **09** (2022) 164, [arXiv:2205.09484 \[hep-ph\]](#).
- [19] P. Coloma, I. Esteban, M. C. Gonzalez-Garcia, L. Larizgoitia, F. Monrabal, and S. Palomares-Ruiz, “Bounds on new physics with data of the Dresden-II reactor experiment and COHERENT,” *JHEP* **05** (2022) 037, [arXiv:2202.10829 \[hep-ph\]](#).
- [20] J. Liao, H. Liu, and D. Marfatia, “Implications of the first evidence for coherent elastic scattering of reactor neutrinos,” *Phys. Rev. D* **106** no. 3, (2022) L031702, [arXiv:2202.10622 \[hep-ph\]](#).
- [21] E. Akhmedov and P. Martínez-Miravé, “Solar $\bar{\nu}_e$ flux: revisiting bounds on neutrino magnetic moments and solar magnetic field,” *JHEP* **10** (2022) 144, [arXiv:2207.04516 \[hep-ph\]](#).
- [22] A. N. Khan, “Neutrino millicharge and other electromagnetic interactions with COHERENT-2021 data,” *Nucl. Phys. B* **986** (2023) 116064, [arXiv:2201.10578 \[hep-ph\]](#).
- [23] V. De Romeri, O. G. Miranda, D. K. Papoulias, G. Sanchez Garcia, M. Tórtola, and J. W. F. Valle, “Physics implications of a combined analysis of COHERENT CsI and LAr data,” *JHEP* **04** (2023) 035, [arXiv:2211.11905 \[hep-ph\]](#).
- [24] P. Coloma, M. C. Gonzalez-Garcia, M. Maltoni, J. a. P. Pinheiro, and S. Urrea, “Constraining new physics with Borexino Phase-II spectral data,” *JHEP* **07** (2022) 138, [arXiv:2204.03011 \[hep-ph\]](#). [Erratum: *JHEP* 11, 138 (2022)].
- [25] C. Giunti and C. A. Ternes, “Testing neutrino electromagnetic properties at current and future dark matter experiments,” *Phys. Rev. D* **108** no. 9, (2023) 095044, [arXiv:2309.17380 \[hep-ph\]](#).
- [26] V. De Romeri, D. K. Papoulias, G. Sanchez Garcia, C. A. Ternes, and M. Tórtola, “Neutrino electromagnetic properties and sterile dipole portal in light of the first solar CE ν NS data,” [arXiv:2412.14991 \[hep-ph\]](#).
- [27] V. De Romeri, D. K. Papoulias, and G. Sanchez Garcia, “Implications of the first CONUS+ measurement of coherent elastic neutrino-nucleus scattering,” *Phys. Rev. D* **111** no. 7, (2025) 075025, [arXiv:2501.17843 \[hep-ph\]](#).
- [28] M. Atzori Corona, M. Cadeddu, N. Cargioli, F. Dordei, and C. Giunti, “Reactor antineutrinos CE ν NS on germanium: CONUS+ and TEXONO as a new gateway to SM and BSM physics,” [arXiv:2501.18550 \[hep-ph\]](#).
- [29] C. Giunti and A. Studenikin, “Neutrino electromagnetic interactions: a window to new physics,” *Rev. Mod. Phys.* **87** (2015) 531, [arXiv:1403.6344 \[hep-ph\]](#).
- [30] K. Fujikawa and R. Shrock, “The Magnetic Moment of a Massive Neutrino and Neutrino Spin Rotation,” *Phys. Rev. Lett.* **45** (1980) 963.
- [31] P. B. Pal and L. Wolfenstein, “Radiative Decays of Massive Neutrinos,” *Phys. Rev.* **D25** (1982) 766.
- [32] K. S. Babu, S. Jana, and M. Lindner, “Large Neutrino Magnetic Moments in the Light of Recent Experiments,” *JHEP* **10** (2020) 040, [arXiv:2007.04291 \[hep-ph\]](#).
- [33] P. Vogel and J. Engel, “Neutrino Electromagnetic Form-Factors,” *Phys. Rev. D* **39** (1989) 3378.
- [34] W. Grimus, M. Maltoni, T. Schwetz, M. A. Tortola, and J. W. F. Valle, “Constraining Majorana neutrino electromagnetic properties from the LMA-MSW solution of the solar neutrino problem,” *Nucl. Phys. B* **648** (2003) 376–396, [arXiv:hep-ph/0208132](#).
- [35] B. C. Canas, O. G. Miranda, A. Parada, M. Tortola, and J. W. F. Valle, “Updating neutrino magnetic moment constraints,” *Phys. Lett. B* **753** (2016) 191–198, [arXiv:1510.01684 \[hep-ph\]](#). [Addendum: *Phys.Lett.B* 757, 568–568 (2016)].

- [36] D. Aristizabal Sierra, O. G. Miranda, D. K. Papoulias, and G. S. Garcia, “Neutrino magnetic and electric dipole moments: From measurements to parameter space,” *Phys. Rev. D* **105** no. 3, (2022) 035027, [arXiv:2112.12817 \[hep-ph\]](#).
- [37] J. Schechter and J. W. F. Valle, “Neutrino Decay and Spontaneous Violation of Lepton Number,” *Phys. Rev. D* **25** (1982) 774.
- [38] W. Grimus and T. Schwetz, “Elastic neutrino electron scattering of solar neutrinos and potential effects of magnetic and electric dipole moments,” *Nucl. Phys. B* **587** (2000) 45–66, [arXiv:hep-ph/0006028](#).
- [39] F. Capozzi and G. Raffelt, “Axion and neutrino bounds improved with new calibrations of the tip of the red-giant branch using geometric distance determinations,” *Phys. Rev. D* **102** no. 8, (2020) 083007, [arXiv:2007.03694 \[astro-ph.SR\]](#).
- [40] C. Giunti, K. Kouzakov, Y.-F. Li, and A. Studenikin, “Neutrino Electromagnetic Properties,” [arXiv:2411.03122 \[hep-ph\]](#).
- [41] P. F. de Salas, D. V. Forero, S. Gariazzo, P. Martínez-Miravé, O. Mena, C. A. Ternes, M. Tórtola, and J. W. F. Valle, “2020 global reassessment of the neutrino oscillation picture,” *JHEP* **02** (2021) 071, [arXiv:2006.11237 \[hep-ph\]](#).
- [42] **LZ** Collaboration, J. Aalbers *et al.*, “First Dark Matter Search Results from the LUX-ZEPLIN (LZ) Experiment,” *Phys. Rev. Lett.* **131** no. 4, (2023) 041002, [arXiv:2207.03764 \[hep-ex\]](#).
- [43] **PandaX** Collaboration, D. Zhang *et al.*, “Search for Light Fermionic Dark Matter Absorption on Electrons in PandaX-4T,” *Phys. Rev. Lett.* **129** no. 16, (2022) 161804, [arXiv:2206.02339 \[hep-ex\]](#).
- [44] **XENON** Collaboration, E. Aprile *et al.*, “Excess electronic recoil events in XENON1T,” *Phys. Rev. D* **102** no. 7, (2020) 072004, [arXiv:2006.09721 \[hep-ex\]](#).